Fiber Optics Tactile Array Probe for Tissue Palpation during Minimally Invasive Surgery

Hui Xie, Hongbin Liu, Shan Luo, Lakmal D. Seneviratne, Kaspar Althoefer

Abstract— **This paper presents a novel fiber optic tactile probe designed for tissue palpation during minimally invasive surgery (MIS). The probe consists of 3×4 tactile sensing elements at 2.6mm spacing with a dimension of 12×18×8 mm^3 allowing its application via a 25mm surgical port. Each tactile element converts the applied pressure values into a circular image pattern. The image patterns of all the sensing elements are captured by a camera attached at the proximal end of the sensor system. Processing the intensity and the area of these circular patterns allows the computation of the applied pressure across the sensing array. Validation tests show that each sensing element of the tactile probe can measure forces from 0 to 1N with a resolution of 0.05 N. The proposed sensing concept is low cost, lightweight, sterilizable, easy to be miniaturized and can be used in magnetic resonance (MR) environments. Experiments using the developed sensor for tissue abnormality detection were conducted. Results show that the proposed tactile probe can accurately and effectively detect nodules embedded inside soft tissue, demonstrating the promising application of this probe for surgical palpation during MIS.**

*Index Terms—*palpation probe, tactile sensor, optical fiber array, MR compatible

I. INTRODUCTION

During open surgery, palpation is a powerful tool in locating subsurface anatomical structures and assessing tissue properties - a process where the clinicians press their fingers on the patient's soft tissue organs to assess tool-tissue interaction forces [1]. The detection of tumors is a good example: certain solid tumors are harder than the surrounding tissue, their presence, sizes, and exact locations can be obtained through tactile feedback, thereby increasing the chances of performing the surgery successfully whilst reducing the error margins. However, in minimally invasive surgery (MIS) – a surgical procedures performed through small incisions which has obtained increasing popularity in operating rooms worldwide, direct manual palpation is not possible, since the surgeon's hand cannot reach into the inside of a patient through the small incisions. It has been shown that MIS offers many advantages compared to traditional, "open" surgery, including reduced tissue trauma, enhanced therapeutic result, and accelerated postoperative recovery.
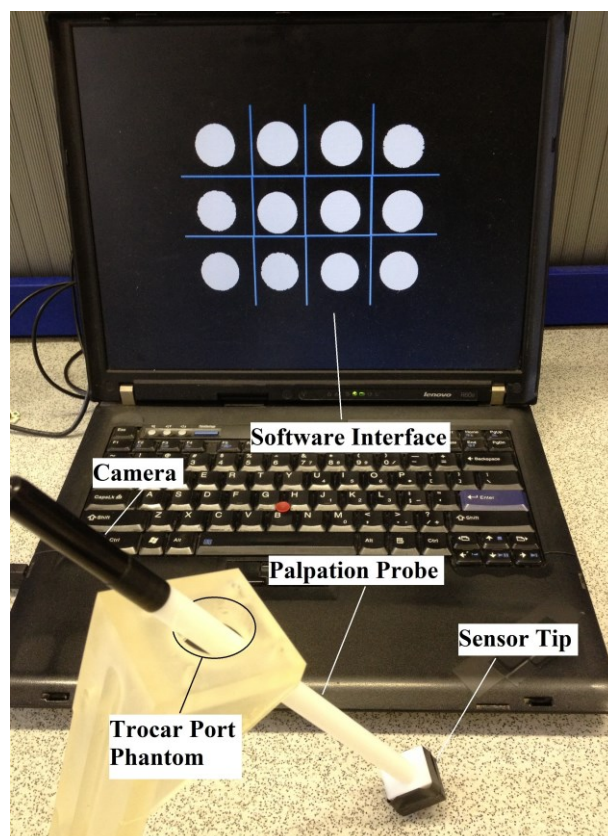
Fig. 1.   Miniature tactile sensor for tissue palpation.

Nevertheless, all these advantages come at the absence of direct tissue interaction and the loss of tactile feedback [2] [3]. During MIS, in order to provide surgeons the substitute of palpation, a popular approach is to develop surgical instruments with force sensing capability to indent, or grasp of a soft tissue [4]. Based on mechanical soft tissue modelling and the measurements of force and tissue local deformation, tissue properties can be identified, providing the surgeon with a better understanding of internal organs during the operation [5]. At present, numerous force and tactile sensing technologies for instrumenting the surgical devices of MIS have been developed [6]. Tholey *et al.* [7] investigated current-based sensing methods in the framework of a specially designed laparoscopic grasper, which proposed a simple way to measure force in MIS. Tadano *et al.* developed a 4 degree-of-freedom pneumatic-driven forceps providing force sensing capabilities based on the measurement of air pressure. In [8], a force-sensitive probe has been created to localize lung tumors based on analysis of tissue stiffness. In [9], a robotic palpation system equipped with force/torque

sensing capability has been developed for examine the prostate gland.

The aforementioned instruments are able to measure the local tissue properties. However it is time consuming to investigate a large tissue area using these devices. To provide a surgeon with the possibility to rapidly investigate the tissue properties of a large area, various palpation have been developed using tactile array sensors to mechanically image the interested tissue area. Based on resistive sensing, Schostek et al. [10] developed a prototype of a MIS grasper which provides both the magnitudes of the applied forces and the distribution of forces. Among certain sensing principles, capacitive-based sensing is comparably efficient for measuring the applied forces and it has been widely applied for palpation. A capacitive tactile array remote palpation system was developed by Howe et al. [11]; this palpation system can measure forces with a high resolution over a range of 0 to 2 N. Commercial capacitive-based tactile array sensors have also been implemented for surgical palpation such as the use of a probe equipped with tactile sensors to identify prostate tumors [12] and to locate the tumor inside lung [13] [14]. The main drawbacks of the resistive-based and the capacitive-based tactile array sensor are problems associated with the sensor sterilization since the sterilization procedure could damage the electronic components of these sensors. In addition these types of sensor are generally not MRI (magnetic resonance imaging) compatible, thus limiting their applications in MRI environment. Since electrical power is not required by the sensing elements, the operations of the piezoelectric-based sensors are considered reliable and the range of its application is greater than it is for other sensors. As an application in MIS, Dargahi et al. [15] developed a micromachined tactile sensor that can be integrated with a jaw of endoscopic graspers. The drawbacks of piezoelectric materials are that they are only sensitive to time-varying forces and are sensitive to changes in temperature.

In the view of the limitations of the above sensing technologies, this paper proposes a fiber optic based tactile array sensor for surgical palpation. The advantages of this method are: the created sensing system is small in size, lightweight, free from electromagnetic interference, water and corrosion resistant and capable to operate in harsh environments. Particularly interesting from the medical point of view is the fact that the sensor whose central elements are optic fibers can be easily sterilized and can be used in MRI scanners. This paper presents a prototype based on our palpation probe concept capable of measuring contact forces and locations using *one* single camera, as shown in Fig.1. This probe can be used during a single-port surgery approach, which has an incision of 3–5cm allowing surgical tools to be inserted and operate. With clear potential of further miniaturization, the probe can fit in multi-port surgery with smaller incisions. The paper describes our most recent achievements on fiber optic based tactile sensor [16]; the original aspects of this paper are further miniaturization, increased sensor sensitivity and crosstalk elimination.

II. METHODOLOGY

Fiber optic based tactile sensing method is a very effective way to equip medical tools working in high intensity electromagnetic field with force measurement. Optical fiber sensor uses four main sensing mechanisms, which are wavelength, phase, polarization and intensity modulation mechanisms. All of these mechanisms consist of a light source, transduction and detection parts. In this paper we use the light intensity modulation method as it is versatile, inexpensive, temperature insensitive and easy to fabricate. Previous work on intensity modulated optical fiber sensors uses a pair of parallel optical fibers [17] with one projecting light onto the other fiber via a flat surface that will move in response to an applied force. Once the distance between the fibers and the surface changes in response to a force, the light intensity received will change and can be measured by a photo sensitive element whose output can be used to quantify the force. Another similar approach is using bent-tip optical fibers proposed in [18] to improve the performance by avoiding the loss of light during transmitting and receiving in the transduction process. Also, the use of a coupler to couple two individual fibers into one single fiber [19] is one of the popular ways to design an optical fiber sensor based on the light intensity modulation principle. It allows for further miniaturization as light is transmitted and received through the same fiber. The disadvantage of using a coupler is the high cost and manufacturing difficulties in displacing the fibers and connecting them.

Most of the existing intensity modulation fiber optic force sensors use individual phototransistors or photodiodes to convert light intensity into voltage and collect through signal acquisition circuits. Then the voltage signal will be calibrated into force information. In this paper, a different method of light intensity modulation is introduced. Instead of using one
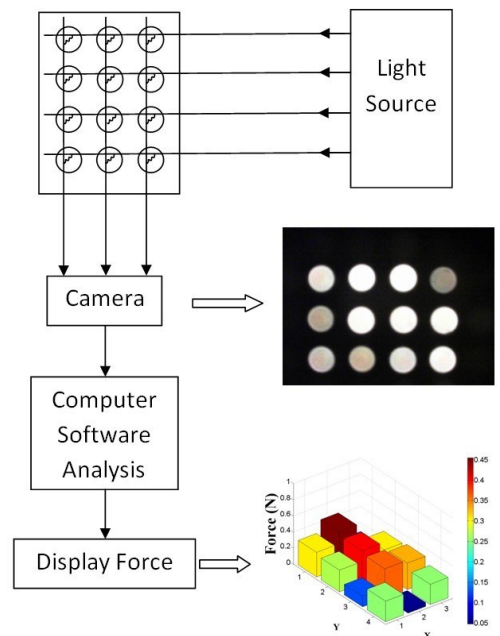

Fig. 2.   Schematic design of proposed tactile sensor using camera.

photo-electronic for each sensing element, *one* single camera is employed to capture and detect the light intensity changes of all sensing elements. The signals are then processed in Matlab/Simulink and converted to force information thus creating a tactile force map.

Fig. 2 shows the schematic design of the presented sensor to explain the sensing methodology. The light source transmits the light to the sensing area, which is a 3 by 4 array with the size of 12×18mm. When force is applied to the sensing element, the displacement change between fiber and mirror is observed by the change of light intensity in the receiving fiber. The light intensity information is then detected as image data by the camera attached at the end of the receiving fiber. The data is then sent to the computer to calculate the contact force and location.

A. Sensor Hardware

Different from previous developed multi-array optic sensors, only two optic fiber bundles are used for developing the described sensor. Inside each bundle there are 16 individual fibers made of polymethyl-methacrylate resin. One fiber bundle is used for transmitting light while the other for receiving light. The fibers are fixed on the supporting base (Fig. 3). The sensor prototype is developed in SolidWorks, as shown in Fig. 4. By using the material of ABS (acrylonitrile butadiene styrene), it has been 3D printed by a rapid prototyping machine using. Between the supporting material and sensing tip, latex rubber is used as the flexible structure. With larger value of applied force, bigger deformation of the rubber will have. The supporting structure is designed with 12 separate grids, to constrain the deforming area, independent from each other. 12 cylinder-like sensing elements with ball shape tip for the contact area are developed for the sensor, to detect applied forces; below each contact area two mirrors are placed at an angle of 90 degree reflecting light from the transmitting fiber to the receiving fiber, which is equivalent to a flat reflective surface with a pair of bent-tip optical fibers set to 90 degree in between, enabling more effective light transmission between fibers. As the sensor detects z-axis force information only, a top layer is designed to constrain the x and y-axis movements of the sensing elements.

B. Sensor Software

Once force has been applied on the tactile sensor, the changes of light intensity corresponded to each sensing element are detected by the camera placed at the end of the receiving fiber bundle. In this prototype, a low cost, high speed USB camera is used to acquire the real-time data shown in Fig. 5 (a) and send the data to PC. The camera image captured at the end of receiving fibers consists of pixels, each pixel represented by red, green and blue (RGB) color components. Employing equation (1), these values can then be converted into grayscale:

$$I = 0.2989\,R + 0.5870\,G + 0.1140\,B. \quad (1)$$

where I is the light intensity, R, G and B represents red, green and blue value of each pixel. The results are shown in Fig. 5 (b).

The grayscale image has many scales of grey including some noises in the sensing system, so we convert it into a binary image which only contains two colors, black and white, utilizing the following equation:

$$n_i = \begin{cases} 0, I_i < I_{threshold} \\ 1, I_i > I_{threshold} \end{cases}, \quad (2)$$

where $I_{threshold}$ is the threshold to eliminate ineffective pixels, n is the value of each pixel. Fig. 5 (c) represents the result.

Then the real-time video data is divided into 12 sections, shown in Fig. 5 (d), each representing one single sensing element. Described in the mathematical model [20], the light intensity received is inversely proportional to the distance change between mirror and fiber, thus proportional to the value of the force applied. That is, increased force will result in brighter video images. The relationship between force f and activated pixels N is given by:
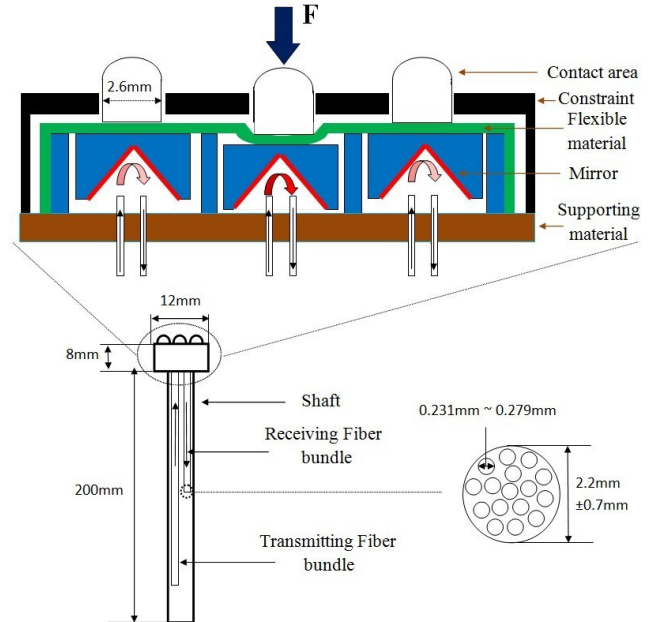
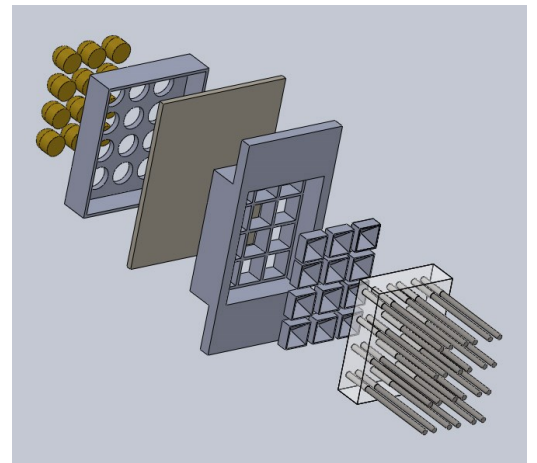

Fig. 3.   Detailed sensor design and assemblies.

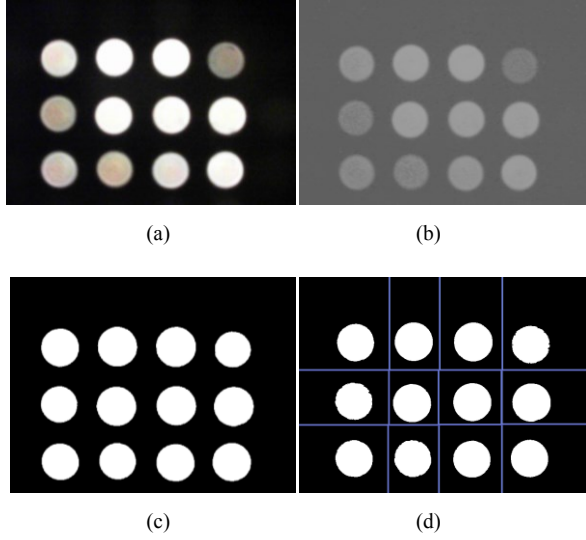Fig. 4.   CAD drawing of proposed sensor.

Fig. 5. Sequence of Image Processing: (a) RGB images captured by camera, (b) RGB2Grayscale conversion, (c) Intensity to binary image, (d) Division into 12 elements.

$$N = \sum_{i=1}^{K} n_i, \qquad (3)$$

$$f \propto N, \qquad (4)$$

where N and K are the total value and number of the pixels in each sensing area, f is the force. The relation between f and N is further investigated and demonstrated in the calibration process reported below.

III. TEST

A Fiber-Lite 3100 Dolan-Jenner Illuminator using an EKZ lamp with cold illumination intensity of 10,000 foot candles is used as the light source. It provides precise four-level solid-state intensity control. Two fiber bundles with outer diameter of 2.2mm ± 0.7mm (including jacket) are used to transmit and receive light. Each bundle has 16 individual optical fibers inside with the core diameter of 0.231mm to 0.279mm. The core refractive index of each fiber is 1.49 and the numerical aperture is 0.50. A high speed, waterproof and low-cost USB endoscope with outer diameter 10mm is installed to transfer the image of light intensity to the computer for further analysis. An ATI Nano 17 Force/Torque sensor together with a National Instruments Data Acquisition Card are used for calibration of the proposed sensor. The sensor calibration set-up is shown in Fig. 6.

A. Calibration

Before using the tactile probe for palpation, calibration is essential. To conduct calibration, the tactile sensor was mounted on a rigid static support and the 12 sensing elements were loaded individually using the ATI Nano 17 Force/Torque sensor, at increments of 0.2 N from 0 N to 1 N. At this stage, the calibration procedure is taken in a non-sterilized environment due to the limitation of calibration equipment. The sterilizable calibration environment will be considered in the future research. The real-time image data is detected and recorded by the camera system and through the image processing procedure, activated pixels are then calculated. The quadratic and linear relationship between the sensor output,
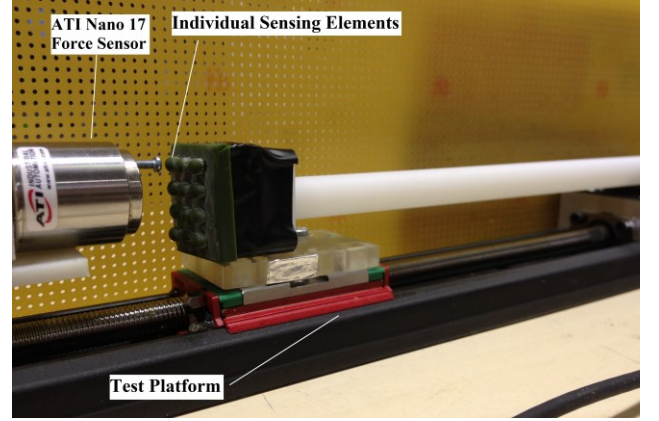

Fig. 6. Sensor Calibration set-up.

which is the pixel number, and applied force are represented by

$$N = \alpha f^2 + \beta f + \gamma, \qquad (5)$$

$$N = \delta f + \varepsilon, \qquad (6)$$

where N is the output of the sensor, f is the force on individual sensing element and α, β, γ, δ, ε are the calibration coefficients, which are listed in Table I and Table II together with respective R-squared values.

TABLE I. COEFFICIENT OF QUADRATIC FITTING CURVE

Sensor Number	Coefficients			
	α	β	γ	R^2
1	-110.1	356.51	5704.2	0.9922
2	-4.4274	1112.2	3622.3	0.985
3	138.76	62.89	6295.5	0.989
4	-4.4274	1112.2	3622.3	0.9835
5	20.008	62.935	6418.9	0.9939
6	-61.194	176.61	6462.7	0.9848
7	241.44	30.802	5981.8	0.9855
8	99.641	-14.12	6661.2	0.9429
9	60.55	74.054	6767.6	0.9948
10	2.9904	18.29	6083.2	0.9945
11	-565.92	1541.1	4045.4	0.9945
12	149.86	2596.1	1879.6	0.9886

TABLE II. COEFFICIENT OF LINEAR FITTING CURVE

Sensor Number	Coefficients		
	δ	ε	R_o^2
1	246.41	5718.8	0.9755
2	1107.8	3622.9	0.9782
3	201.65	6277	0.9506
4	1107.8	3622.9	0.9835
5	82.942	6416.2	0.989
6	115.41	6470.8	0.9617
7	272.24	5949.6	0.9235
8	85.521	6647.9	0.8451
9	134.6	6759.5	0.978
10	39.223	6055.3	0.9823
11	975.21	4120.8	0.9667
12	2746	1859.6	0.9884

From the Table I and II it can be concluded that quadratic fitting for each sensing element have higher R-squared values than linear fitting. While in Table II it also shows the sensor has a reasonable linearity between sensor output and applied force with most of the R-squared values close to 1. Fig. 7 shows the relations between activated pixels and applied forces of sensing element 1 for both linear and quadratic fitting. Each sensing element has been tested 10 times and the standard deviations are seen by the error bars corresponding to every increment.

B. Experimental Results of Tissue Palpation

The tissue palpation experiment was conducted using a planar surface silicone phantom tissue with a 10mm spherical nodule embedded at a depth of 6mm as shown in Fig. 8 (a). The tactile probe was maneuvered down vertically against the phantom tissue surface to an indentation depth of 3mm. Two different areas, A and B, of the tissue is tested, area A
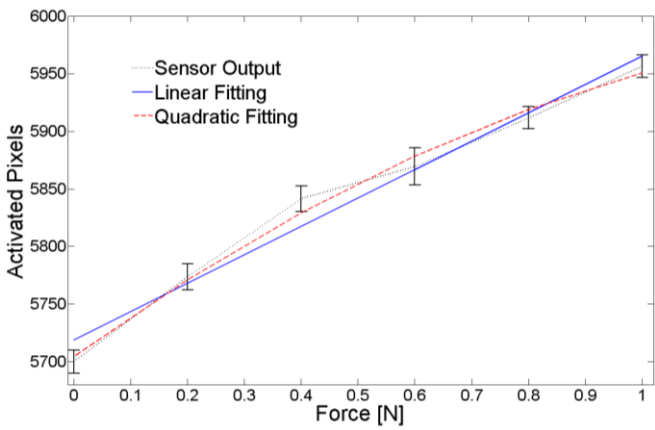

Fig. 7. Measured output responses of sensing element 1 to the normal force applied.

(a)   (b)
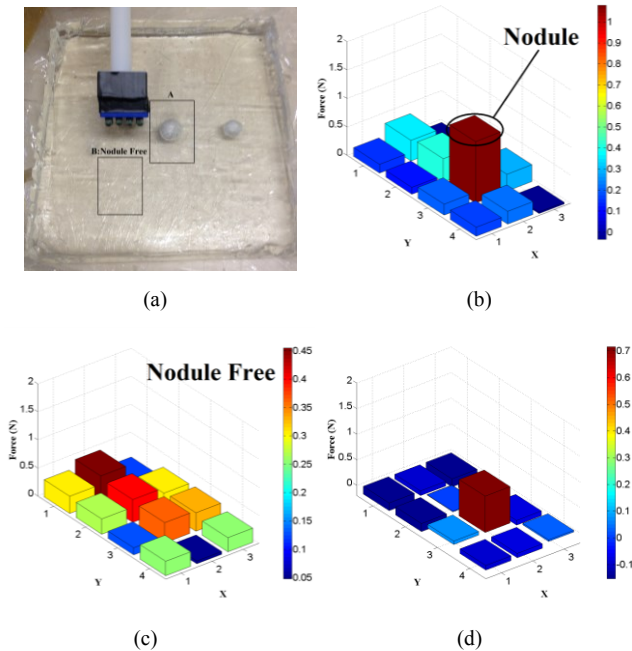

(c)   (d)

Fig. 8. (a) Palpation test on silicone phantom tissue, (b) Test results on area A, (c) Test results on area B, (d) Effective stiffness distribution map by compare test results on two areas.

includes the nodule while area B does not. The palpation process is repeated ten times. The responses of the sensor output after palpation in the two areas are shown in Fig. 8 (b) and (c). From the results, outputs of each sensing element in nodule free area varies mostly in the range of $0 - 0.4$ N. While in the nodule embedded area, outputs of the sensing elements in contact with nodule exceed the value 0.8N. Then from the force distribution map we can tell the location of the hard nodule. To eliminate noise from normal tissue feedback and make a more clear view of the nodule location, a normalized nodule map of Fig. 8 (d) is obtained by subtracting Fig. 8 (c) from Fig. 8 (b).

The results also show that when one sensing element is in contact with a hard nodule, it relieves the force applied on its surrounding sensing elements caused by the compression from the silicone phantom tissue. While compared to the nodule detecting force, these noise levels are kept in an acceptable range.

After evaluating the performance on silicone phantom tissue, a lamb kidney with an embedded nodule was tested. The nodule has a diameter of 8mm and is approximately 3-4 times as stiff as the lamb kidney. It was buried close to the kidney surface, shown in Fig. 9 (a). The developed tactile probe is usable on both flat and non-flat surfaces, while in the latter case the probe needs to be positioned according to the geometry of the objects. During the test, three flat areas of the lamb kidney for palpation were used, with area B embedded with a hard nodule while area A and C are nodule free which are also both flat. Then, the probe was vertically moved down up to a predefined indentation depth on all three areas. The test results during the palpation process are shown in Fig. 9 (b). By combining sensor outputs in all three areas, the tactile image of the palpation area is created. From the image, the sensor output in the central area of B exceeds 0.3 N while others are near 0.1 N, which indicates the location of the hidden nodule. Compared to the silicone phantom tissue, lamb kidney is softer and easy to be damaged. This requires
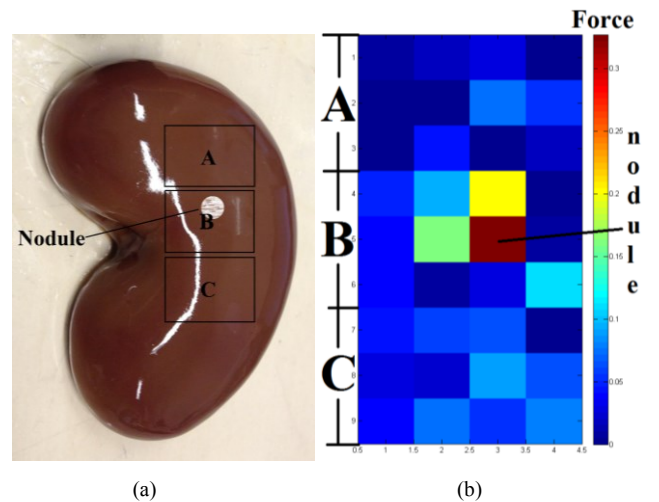

(a)   (b)

Fig. 9. (a) Lamb kidney sample with invisible nodule buried in area B, (b) Test results of the tactile sensor by palpating on three areas.

the palpation device to be flexible and sensitive, and the proposed one shows its capability of conducting accurate and effective tissue palpation for tissue abnormality detection.

IV. DISCUSSION AND CONCLUSION

This paper presents a laboratory prototype tactile probe for palpation during minimally invasive surgery. It can measure the normal force and its distribution over the sensor's area based on light intensity modulation in order to detect abnormal tissue during palpation both in an open surgery and during MIS. The force is detected and calculated by a camera system using a pixel-based method. As no metallic material and no electrical signals are used in the sensing area, this sensor has good potential to be used in an MRI environment. Test results have shown the feasibility of the sensing approach together with the accuracy of the probe in detecting nodules. The sensor also has many advantages associated with employing fiber optics, e.g. light-weight, not being susceptible to electromagnetic noise and being easily sterilized – the basic requirement for a medical tool. Only *one* camera was used in the detection system, which provides not only potential for low cost production but also a good sensing resolution.

Future research will focus on further miniaturization in order to fit through even smaller trocar ports during MIS and on extending the tactile spatial resolution and possibly adding the measurement of shear forces.

REFERENCES

[1] T. R. Coles, D. Meglan, S. Member, and N. W. John, "The Role of Haptics in Medical Training Simulators : A Survey of the State of the Art," *Haptics, IEEE Transactions* vol. 4, no. 1, pp. 51–66, 2011.

[2] J. Rosen, B. Hannaford, M. P. MacFarlane, and M. N. Sinanan, "Force controlled and teleoperated endoscopic grasper for minimally invasive surgery--experimental performance evaluation.," *IEEE transactions on bio-medical engineering*, vol. 46, no. 10, pp. 1212–21, Oct. 1999.

[3] H. Liu, D. P. Noonan, B. J. Challacombe, P. Dasgupta, L. D. Seneviratne, and K. Althoefer, "Rolling mechanical imaging for tissue abnormality localization during minimally invasive surgery.," *IEEE transactions on bio-medical engineering*, vol. 57, no. 2, pp. 404–14, Feb. 2010.

[4] G.-P. Haber, M. a White, R. Autorino, P. F. Escobar, M. D. Kroh, S. Chalikonda, R. Khanna, S. Forest, B. Yang, F. Altunrende, R. J. Stein, and J. H. Kaouk, "Novel robotic da Vinci instruments for laparoendoscopic single-site surgery.," *Urology*, vol. 76, no. 6, pp. 1279–82, Dec. 2010.

[5] M. V. Ottermo, O. Stavdahl, and T. a. Johansen, "Palpation instrument for augmented minimally invasive surgery," *2004 IEEE/RSJ International Conference on Intelligent Robots and Systems (IROS) (IEEE Cat. No.04CH37566)*, vol. 4, pp. 3960–3964, 2004.

[6] P. Puangmali, K. Althoefer, L. D. Seneviratne, D. Murphy, and P. Dasgupta, "State-of-the-Art in Force and Tactile Sensing for Minimally Invasive Surgery," *IEEE Sensors Journal*, vol. 8, no. 4, pp. 371–381, Apr. 2008.

[7] K. Tadano and K. Kawashima, "Development of 4-DOFs forceps with force sensing using pneumatic servo system," *Proceedings 2006 IEEE International Conference on Robotics and Automation, 2006. ICRA 2006.*, no. May, pp. 2250–2255, 2006.

[8] G. L. Mccreery, A. L. Trejos, M. D. Naish, R. V Patel, and R. A. Malthaner, "Feasibility of locating tumours in lung via kinaesthetic feedback," *The International Journal of Medical Robotics and Computer Assisted Surgery* 4, no. 1 no. January, pp. 58–68, 2008.

[9] B. Ahn, Y. Kim, C. K. Oh, and J. Kim, "Robotic palpation and mechanical property characterization for abnormal tissue localization.," *Medical & biological engineering & computing*, vol. 50, no. 9, pp. 961–71, Sep. 2012.

[10] D. A. Kontarinis and J. S. Son, "Remote Palpation Technology," *Engineering in Medicine and Biology Magazine, IEEE,* no. June, 1995.

[11] M. Biehl and J. Meyer, "Vibrotactite Palpation Instrument for Use in Minimal Invasive Surgery," *In Engineering in Medicine and Biology Society, 1996. Bridging Disciplines for Biomedicine. Proceedings of the 18th Annual International Conference of the IEEE,* vol. 1, pp. 179–180.

[12] V. Egorov, S. Ayrapetyan, and A. P. Sarvazyan, "Prostate mechanical imaging: 3-D image composition and feature calculations.," *IEEE transactions on medical imaging*, vol. 25, no. 10, pp. 1329–40, Oct. 2006.

[13] A. P. Miller, W. J. Peine, J. S. Son, and Z. T. H. M. D, "Tactile Imaging System for Localizing Lung Nodules during Video Assisted Thoracoscopic Surgery 1," ." *In Robotics and Automation, 2007 IEEE International Conference on,* no. April, pp. 10–14, 2007.

[14] a. L. Trejos, J. Jayender, M. T. Perri, M. D. Naish, R. V. Patel, and R. a. Malthaner, "Robot-assisted Tactile Sensing for Minimally Invasive Tumor Localization," *The International Journal of Robotics Research*, vol. 28, no. 9, pp. 1118–1133, May 2009.

[15] S. J. Mihailov, "Fiber Bragg grating sensors for harsh environments.," *Sensors (Basel, Switzerland)*, vol. 12, no. 2, pp. 1898–918, Jan. 2012.

[16] H. Xie, A. Jiang, L. Seneviratne, and K. Althoefer, "Pixel-based Optical Fiber Tactile Force Sensor for Robot Manipulation," In *Sensors, IEEE*, 2012.

[17] P. D. Goodyer, J. C. Fothergill, N. B. Jones, and C. D. Hanning, "The Design of an Optical Fiber Pressure Transducer for Use in the Umer Airways," *IEEE Trans. Biomed. Eng.* vol. 43, no. 6, pp. 0–6, 1996.

[18] H. Liu, P. Puangmali, K. a. Althoefer, and L. D. Seneviratne, "Experimental study of soft tissue recovery using optical fiber probe," *2007 IEEE/RSJ International Conference on Intelligent Robots and Systems*, pp. 516–521, Oct. 2007.

[19] P. Polygerinos, T. Schaeffter, L. Seneviratne, and K. Althoefer, "A fibre-optic catheter-tip force sensor with MRI compatibility: a feasibility study.," *Conference proceedings : ... Annual International Conference of the IEEE Engineering in Medicine and Biology Society. IEEE Engineering in Medicine and Biology Society. Conference*, vol. 2009, pp. 1501–054, Jan. 2009.

[20] P. Puangmali, K. Althoefer, and L. D. Seneviratne, "Mathematical Modeling of Intensity-Modulated Bent-Tip Optical Fiber Displacement Sensors," *IEEE Transactions on Instrumentation and Measurement*, vol. 59, no. 2, pp. 283–291, Feb. 2010.